Steady-State Kinetics and Inhibitor Binding of 3-Deoxy-D-*arabino*-heptulosonate-7-phosphate Synthase (Tryptophan sensitive) from *Escherichia coli*†

James P. Akowski‡ and Ronald Bauerle*

Department of Biology, University of Virginia, Charlottesville, Virginia 22903-2477

Received May 14, 1997; Revised Manuscript Received September 23, 1997⊗

ABSTRACT: The tryptophan-inhibited 3-deoxy-D-*arabino*-heptulosonate-7-phosphate synthase [DAHPS-(Trp)] of *Escherichia coli* was analyzed with respect to steady-state kinetics and tryptophan binding. DAHPS(Trp) is one of three differentially regulated isoforms that catalyze the first step of aromatic biosynthesis, the condensation of phospho*enol*pyruvate and erythrose-4-phosphate to form 3-deoxy-D-*arabino*-heptulosonate-7-phosphate. The DAHP synthase isozymes are metalloproteins, being activated *in vitro* by a variety of divalent metals. Both catalytic activity and substrate affinity are dependent on the species of activating metal ion. We report here kinetic and binding studies of metal-homogeneous (Mn^{2+}-activated) DAHPS(Trp). The homodimeric enzyme had an apparent k_{cat} of 21 s^{-1} and displayed sigmoidal kinetics with respect to both substrates. The $S_{0.5}$ was 35 μM for erythrose-4-phosphate and 5.3 μM for phospho*enol*pyruvate. Equilibrium binding studies with radiolabeled tryptophan demonstrated two independent inhibitor binding sites per enzyme dimer, with K_d^{Trp} of 1 μM. L-Tryptophan binding decreased k_{cat}, increased affinity for both substrates, decreased positive homotropic cooperativity for both substrates and activated the enzyme at low concentrations of erythrose-4-phosphate. The results suggest an inhibition mechanism analogous to system C5 hyperbolic mixed-type inhibition with respect to erythrose-4-phosphate and partial noncompetitive inhibition with respect to phospho*enol*pyruvate.

The first step in the biosynthesis of aromatic compounds, the condensation of erythrose-4-phosphate (E4P)[1] and phospho*enol*pyruvate (PEP) to form 3-deoxy-D-*arabino*-heptulosonate 7-phosphate (DAHP), is catalyzed by DAHP synthase (EC 4.1.2.15). In *Escherichia coli*, there are three DAHP synthase isoforms, each specifically feedback-inhibited by the one of the three aromatic amino acids (*1*). Feedback inhibition of the *E. coli* isozymes represents the principal means by which metabolite flow into aromatic synthesis is regulated (*2*). While the tyrosine- and phenylalanine-sensitive isozymes DAHPS(Tyr) and DAHPS(Phe) are inhibited to greater than 95% (*3*), the tryptophan-sensitive isozyme DAHPS(Trp) is maximally inhibited to only 56−70% (*4*−*6*). Thus, the *E. coli* DAHP synthases provide an excellent model system to investigate the evolutionary mechanisms by which highly homologous enzymes have attained the ability to respond to different regulatory effectors.

The *E. coli* DAHP synthases have an absolute requirement for divalent metal cations, being activated *in vitro* by a variety of divalent metals, including Fe^{2+}, Mn^{2+}, Cd^{2+}, Ni^{2+}, Cu^{2+}, Co^{2+}, and Zn^{2+} (*7*). The nature of the metal activator *in vivo* has not yet been established unequivocally, but there is evidence for both Fe^{2+} and Cu^{2+} (*6*−*8*). Both catalytic activity and E4P affinity vary greatly depending on the species of the activating metal (*7*). Thus, a meaningful kinetic treatment of the DAHP synthases requires conditions of strict metal-homogeneity, which has not been the case in most earlier studies. We report here the results of a steady-state kinetic analysis of the activity and feedback inhibition of metal-homogenous (Mn^{2+}-activated) DAHPS(Trp).

MATERIALS AND METHODS

Host/Vector System for DAHPS(Trp) Expression. Expression plasmid pCHA3 was constructed by subcloning the *E. coli aroH* coding sequence behind the *tac* promoter in the high copy number, ampicillin resistance phagemid vector, pttS9 (*7*). The pCHA3 plasmid was maintained in *E. coli* host strain CB735 [C600 *leu thi1* Δ(*gal-aro*G-*nad*A)50 *aro*F::*cat*(Cm^r) Δ*aro*H::Kan^r *recA1*/F′(*lacI*^{q} ZΔM15 *pro*AB Tn10-(Tet^r)] in which the three chromosomal DAHP synthase genes (*aro*F, *aro*G, and *aro*H) had been inactivated by deletion and/or interruption by an antibiotic resistance cassette, as indicated.

Media. Expression medium consisted of K_2HPO_4 (13 g/L), KH_2PO_4 (4.5 g/L), $(NH_4)_2SO_4$ (1 g/L), $MgSO_4 \cdot 7H_2O$ (0.1 g/L), glucose (5 g/L), casamino acids (Difco) (1 g/L), nicotinic acid (12.5 mg/L), thiamine (16.8 mg/L), leucine (39.5 mg/L), threonine (35.5 mg/L), tryptophan (100 mg/L), phenylalanine (100 mg/L), tyrosine (100 mg/L), *p*-hydroxybenzoic acid (20 mg/L), *p*-aminobenzoic acid (20 mg/L) and ampicillin (50 mg/L).

Chemicals and Enzymes. Metals were removed from water, BTP buffer, and substrate and amino acid solutions

† This research was supported by Grant GM35889 from the National Institute of General Medical Sciences, National Institutes of Health.

* To whom correspondence should be addressed.

‡ Present address: Center for Mechanistic Biology, Argonne National Laboratory, Argonne, IL 60439.

⊗ Abstract published in *Advance ACS Abstracts,* November 15, 1997.

[1] Abbreviations: BTP, 1,3-bis[tris(hydroxymethyl)methylamino]-propane; E4P, D-erythrose-4-phosphate; R5P, D-ribose-5-phosphate; PEP, phospho*enol*pyruvate; DAHP, 3-deoxy-D-*arabino*-heptulosonate 7-phosphate; DAHPS, DAHP synthase; DTT, dithiothreitol; BPD buffer, BTP+PEP+DTT buffer; EDTA, ethylenediaminetetraacetic acid.

S0006-2960(97)01135-5 CCC: $14.00

with Chelex 100 (Bio-Rad Laboratories) as recommended by the manufacturer. PEP (monocyclohexylammonium salt) solutions were quantified after Chelex treatment both spectrophotometrically ($\epsilon_{232nm} = 2800\ M^{-1}\ cm^{-1}$) and enzymatically using purified DAHPS(Trp) in the presence of excess E4P (sodium salt). E4P solutions were quantified after Chelex treatment using purified DAHPS(Trp) in the presence of excess PEP. L-Tryptophan solutions were quantified spectrophotometrically ($\epsilon_{280nm} = 5600\ M^{-1}\ cm^{-1}$) after Chelex treatment. The effectiveness of the Chelex treatment has been verified by atomic absorption spectrometry (*7*). High-purity DTT (American Bioanalytical) and $MnCl_2$ (Malinckrodt, >99.97%) were used without further treatment. BPD buffer consisted of 40 mM BTP (pH 7.0 at 25 °C), 100 μM PEP, 500 μM DTT.

Purification of DAHPS(Trp) Apoenzyme. The purification of DAHPS(Trp) was based on the method of Ray and Bauerle (*6*) with modifications. The following protocol is for 1 L of bacterial culture, which routinely yielded 15−20 mg of purified enzyme. CB735/pCHA3 was grown in expression medium at 37 °C with vigorous shaking in a 2 liter baffled flask. Expression of the *aroH* gene was induced by the addition of 0.5 mM dioxane-free isopropyl-β-D-thiogalactoside (Ambion) at mid-logarithmic phase ($A_{550nm} = 0.5$). After incubation for an additional 6 h (final $A_{550nm} = 1.2-1.6$), cells were harvested by centrifugation and washed with 1 vol of cold 0.9% NaCl. Subsequent manipulations were carried out at 0−4 °C except for anion-exchange chromatography, which was performed at room temperature. Drained cell pellets were resuspended in 4 mL of BPD/g of wet cells and sonified in 6 mL batches at 70 W for 45 s in ice-jacketed 50 mL stainless-steel beakers. Cell debris was removed by centrifugation at 50000*g* for 30 min. One-tenth the volume of 20% streptomycin sulfate was added dropwise to the supernatant with stirring. After 10 min, the precipitate was removed by centrifugation at 12000*g* for 10 min. Cold acetone was added dropwise to the supernatant with stirring to a final concentration of 25% (v/v). After 15 min, the precipitate was collected by centrifugation at 12000*g* for 20 min, drained well, and then dissolved in 2.5 mL of BPD + 250 mM KCl. After dissolution of the pellet, the extract was diluted with 2.5 mL of BPD (to reduce the concentration of KCl) and clarified by centrifugation at 12000*g* for 5 min followed by centrifiltration through a 0.22 μm cellulose acetate filter. The filtrate was applied to a Mono-Q HR 10/10 anion-exchange column (10 mm × 10 cm) (Pharmacia LKB) equilibrated with 10 mM BTP (pH 7.0) containing 0.5 mM DTT. The column was developed with a 240 mL linear gradient of 0 to 500 mM KCl in the same buffer at a flow rate of 4 mL/min. Protein elution was monitored at A_{280nm}. DAHPS(Trp) eluted as the major peak at 21−23 min (~175 mM KCl). PEP (100 μM) and DTT (500 μM) were added immediately to fractions containing DAHP synthase activity.

Endogenous metals were removed from the purified DAHPS(Trp) as previously described (*7*) with the following modifications. Purified enzyme was dialyzed for 12 h against 400 mL of 40 mM Chelex-treated BTP containing 1 mM EDTA and 0.5 mM DTT, followed by dialysis for 6 h against two changes of metal-free BPD. Inclusion of DTT in the buffers prevented precipitation of the metal-free enzyme. Before use, dialysis tubing and closures were boiled for 10 min in 2% sodium bicarbonate, 1 mM EDTA, 1 mM ethylene glycol bis(β-aminoethyl ether) *N*,*N*,*N*′,*N*′-tetraacetic acid, rinsed with deionized H_2O, boiled 10 min in deionized H_2O, and stored in 1 mM EDTA. The final enzyme preparation was >95% homogeneous as judged by Coomassie blue staining of SDS−PAGE gels, with the major contaminant being the 31 kDa proteolytic fragment of DAHPS(Trp) identified in earlier work (*6*). Activities in the absence of added metal were usually <1−2% (and always <5%) of those in assays containing Mn^{2+}. There was no consumption of PEP by the purified enzyme in the absence of E4P.

Assay of DAHPS Activity. DAHP synthase activity was assayed spectrophotometrically by monitoring the rate of disappearance of PEP at 232 nm using a Varian DMS200 dual-beam spectrophotometer set with a slit width of 1 nm and smoothing constant of 0.2 s (*6*). Standard 1.0 mL reaction mixtures contained 100 mM BTP, 150 μM PEP, 300 μM E4P, and 50 μM $MnCl_2$. Reactions were followed in 1 cm square quartz cuvettes maintained at 25 °C in a water-jacketed cuvette holder. Cuvettes were soaked overnight in 1 N NaOH followed by 20% H_3PO_4 to remove trace metals and all solutions were pipetted with metal-free pipette tips (Bio-Rad Laboratories).

For kinetic experiments, substrate and inhibitor concentrations were varied as indicated. When PEP was the variable substrate, E4P was held constant at 300 μM (~9 times K_m); when E4P was the variable substrate, PEP was at 150 μM (~28 times K_m). Control experiments using substrate concentrations up to four times these levels confirmed that these concentrations were saturating and also eliminated the possibility of substrate inhibition. Reactions were initiated by the addition of 10 μL of E4P solution and were routinely performed in duplicate. Initial velocities (v_o) were calculated by averaging reaction rates determined at successive 6 s intervals. For graphical analysis of the data, substrate concentrations were calculated as the mean concentration of substrate present during the assay period, as described by Lee and Wilson (*9*). Kinetic parameters were calculated by nonlinear regression analysis of velocity curves (initial velocity *v*s mean substrate concentration) using SigmaPlot, version 5.0, computer software (Jandel Corp.). V_{max} and n_{app} (the apparent Hill coefficient) were determined by nonlinear regression analysis of velocity curves using the Hill equation, where $v_o = V_{max}[S]^{n_{app}}/(K' + [S]^{n_{app}})$ (*10*). $S_{0.5}$ (*i.e.*, the concentration of substrate resulting in one-half V_{max}) was derived using the relationship $S_{0.5} = (K')^{1/n_{app}}$ (*10*).

Protein Quantification. Measurement of protein concentration with the Bio-Rad protein reagent [which overestimates the concentration of purified enzyme by a factor of 1.56 (*7*)] was used to determine an extinction coefficient of 90 500 $M^{-1}\ cm^{-1}$ for DAHPS(Trp) apoenzyme at 280 nm. Absorbance at 280 nm was subsequently used to determine enzyme concentration. Concentrations of the DAHPS(Trp) dimer are indicated as micromolar and monomer subunit as micronormal.

Tryptophan Binding. Equilibrium binding studies were carried out by ultrafiltration (*11*) using Centrifree micropartition centrifugation devices (Amicon Inc.) and ^{14}C-labeled tryptophan. L-[Side chain-3-^{14}C]tryptophan (5 nCi, 53.8 Ci/mol) was added to various concentrations of unlabeled Trp and enzyme to produce a 200 μL solution containing 40 mM BTP (pH 7.0), 100 μM PEP, 50 μM $MnCl_2$, and 5 μN enzyme (subunit concentration). The solution was centrifuged in the micropartition device for 2.5 min at 1240*g* at

room temperature (25 °C) for the time required to produce approximately 70 μL filtrate. A 50 μL portion of filtrate was used for the determination of radioactivity by liquid scintillation counting. The amount of radioactivity bound by the partitioned enzyme was determined by comparison of sample filtrate with the filtrate from mock assays containing no enzyme and various concentrations of unlabeled Trp.

RESULTS

Steady-State Kinetics. Kinetic parameters, derived from steady-state, pseudo-single-substrate, initial velocity assays, were determined for DAHPS(Trp) with Mn^{2+} as activating metal. Mn^{2+} was used as cofactor because, of all the activating divalent metal ions, it supports the highest k_{cat} (*7*). The velocity curves for both E4P and PEP were sigmoidal. The non-Michaelis−Menten character is readily apparent in both Lineweaver−Burk and Eadie−Hofstee plots of the data (Figure 1). The k_{cat} of the enzyme, derived from these data, was 20.6 ± 1.1 s^{-1}; the $S_{0.5}$ for E4P was 35 μM and for PEP was 5.3 μM. Apparent Hill coefficients (n_{app}), determined by nonlinear regressional curve fitting of the data to the Hill equation, were 2.6 for E4P and 2.2 for PEP (Figure 2).

Kinetics of Tryptophan Inhibition. As had been observed in earlier studies with crude and partially purified preparations under conditions of metal heterogeneity (*4, 5, 12*), feedback inhibition of purified Mn^{2+}-DAHPS(Trp) was partial, with maximum inhibition at 61% (data not shown). The concentration of tryptophan required for half-maximal inhibition ($I_{0.5}$ = 30.5%) was 1.4 μM. Graphical analysis of the data using a Hill plot modified to accommodate partial inhibition (*13*) revealed no cooperativity in tryptophan feedback (Figure 3).

The results of the kinetic analysis of tryptophan inhibition at varying concentrations of E4P and PEP are presented as Lineweaver−Burk plots in Figure 4. With E4P as limiting substrate, increasing concentrations of tryptophan led to decreases in V_{max} and $S_{0.5}$ (Figure 4a and Table 1). Furthermore, at low concentrations of E4P, enzymatic activity *increased* in the presence of tryptophan. The concentration of E4P at which tryptophan made the transition from activator to inhibitor decreased as the concentration of tryptophan increased. It was also found that, as the concentration of tryptophan increased, n_{app} for E4P, determined by Hill plots of the data (not shown), decreased almost 2-fold (Table 1). This unusual combination of inhibitor effects, *i.e.*, increased substrate affinity and decreased catalytic activity and activation at low substrate concentrations, are characteristic of System C5 hyperbolic mixed-type inhibition of Segel (*10*).

With respect to the second substrate, PEP, values for V_{max} and n_{app} decreased with increasing tryptophan concentrations, although not to the same extent as with E4P (Figure 4b and Table 1). However, $S_{0.5}$ was generally unchanged, and activation by tryptophan at low substrate concentrations, as had been observed with E4P, was not apparent with PEP.

Tryptophan Binding. The affinity of the enzyme for tryptophan was determined by direct-binding experiments using partition ultrafiltration, as described in Materials and Methods. The double-reciprocal plot of the data (Figure 5) indicated the existence of one tryptophan binding site per enzyme subunit. There was no apparent cooperativity in

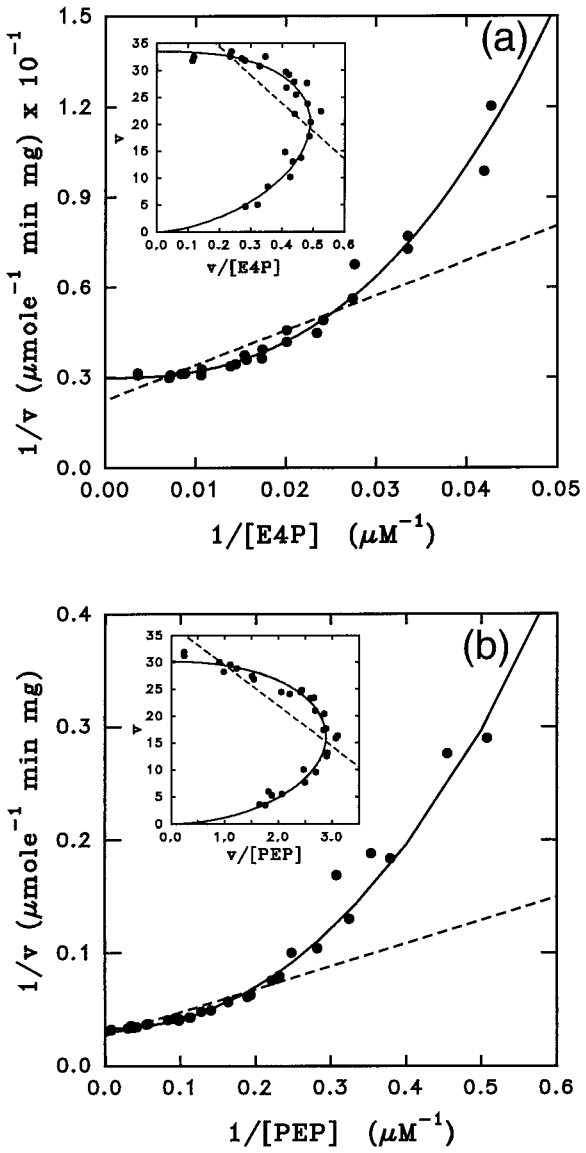

FIGURE 1: Lineweaver−Burk plots of DAHPS(Trp) initial velocity data with (a) erythrose-4-phosphate and (b) phospho*enol*pyruvate as variable substrate. Inserts display the same data as Eadie−Hofstee plots. Conditions were as described in Materials and Methods. Nonvaried PEP was at 150 μM and nonvaried E4P at 300 μM. DAHPS(Trp) was at 22 nM. Solid lines represent curves with the data fitted to the Hill equation by nonlinear regression analysis. Dotted lines represent curves with the data fitted to the Michaelis−Menten equation.

tryptophan binding. The dissociation constant for tryptophan (K_d^{Trp}), determined by nonlinear regression analysis using the Langmuir isotherm (*14*), was 0.97 μM.

Substrate Specificity of DAHPS(Trp). The possibility that DAHPS(Trp) might exhibit substrate ambiguity with respect to E4P was examined by replacing E4P in the reaction mixture with a variety of compounds of related structure, including D-glucose-6-phosphate, D-arabinose, DL-glyceraldehyde, D-erythrose, glycolaldehyde, DL-glyceraldehyde-3-phosphate, and D-ribose-5-phosphate. All were tested at 600 μM (DL-isomeric mixtures were at 1.2 mM) under otherwise standard reaction conditions. Of these, only ribose-5-phosphate (R5P) was found to be utilized by the enzyme. The rate of R5P utilization was slow, about 2% of that observed in control reactions with E4P. Possible contamination of the R5P reagent with small amounts of E4P was excluded by extensive incubation in the presence of enzyme

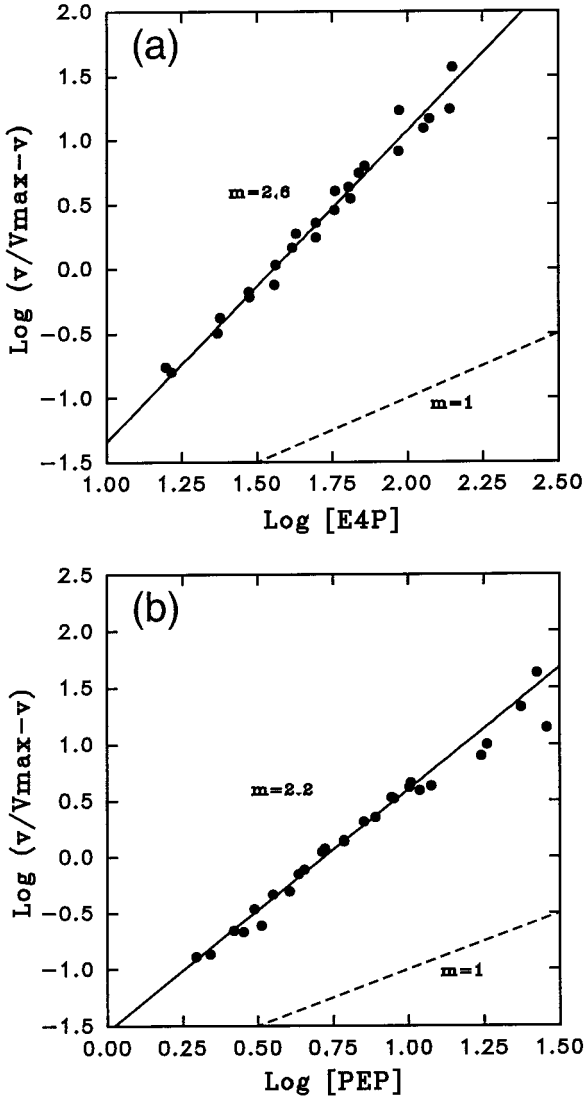

FIGURE 2: Hill plots of DAHPS(Trp) initial velocity data with (a) erythrose-4-phosphate and (b) phospho*enol*pyruvate as variable substrate. The curves are replots of the data of Figure 1.

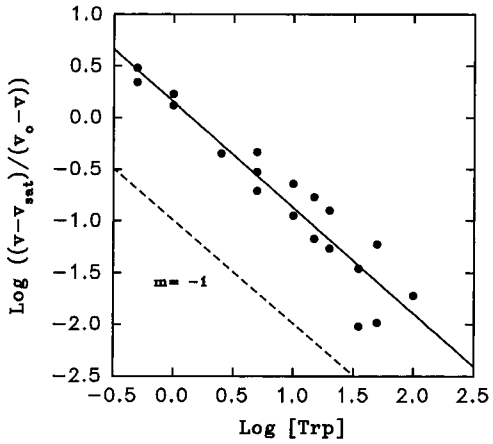

FIGURE 3: Modified Hill plot of DAHPS(Trp) tryptophan inhibition. The plot was modified according Atkinson (*13*). v and v_o are the initial velocities in the presence and absence of tryptophan, respectively; v_{sat} is the initial velocity in the presence of saturating tryptophan. $v_o = 46.5$ nmoles/min; $v_{sat} = 18$ nmol/min. The dashed line is drawn with a slope of −1.0.

and excess PEP, which resulted in >65% consumption of the R5P. No attempt was made to recover and characterize the product of the R5P reaction.

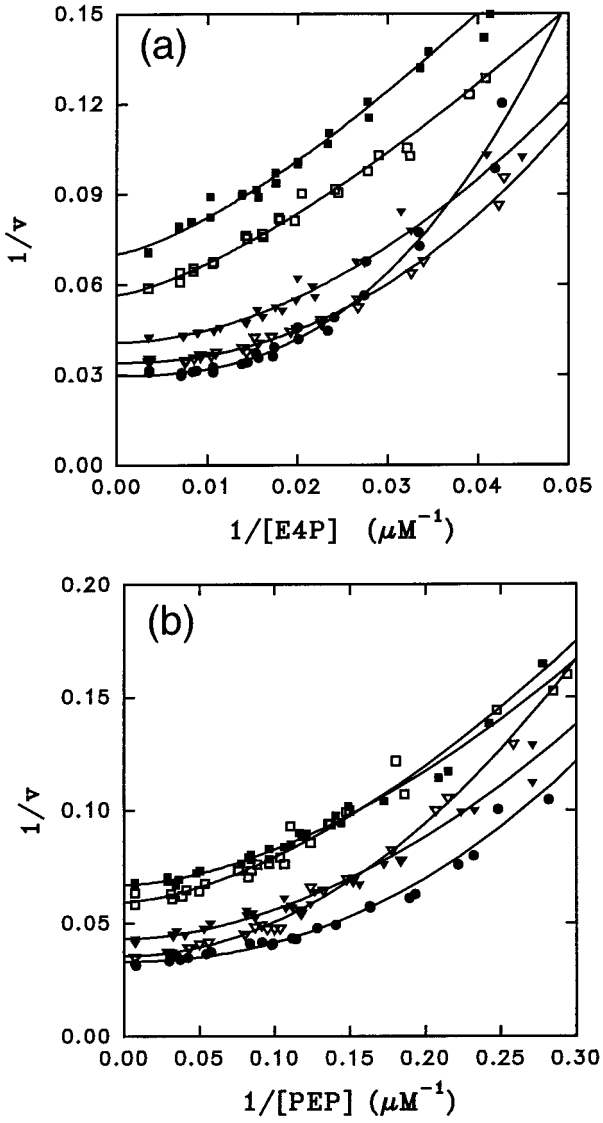

FIGURE 4: Lineweaver−Burk plots of tryptophan inhibition of DAHPS(Trp) with (a) erythrose-4-phosphate and (b) phospho-*enol*pyruvate as varied substrate. Conditions were as described in Figure 1. Tryptophan concentrations were 0 μM (●), 0.3 μM (△), 1.0 μM (▲), 5.0 μM (□), and 20 μM (■).

DISCUSSION

Substrate Kinetics. The sigmoidal velocity curves observed here with Mn^{2+}-DAHPS(Trp) demonstrate that the enzyme does not obey simple Michaelis-Menten kinetics. Similar results have been reported with other DAHP synthases (*7*, *15*−*16*). DAHPS(Trp), a homodimeric protein, presumably possesses one catalytic site per subunit, as has been shown with the tetrameric DAHPS(Phe) (*17*). However, the n_{app} values obtained here for DAHPS(Trp) [*i.e.*, 2.6 for E4P and 2.2 for PEP (Table 1)] exceed the number of substrate binding sites ($n = 2$). Thus, the observed positive cooperativity must derive from means other than, or perhaps in addition to, interactions affecting substrate binding. This might also be the case with DAHPS(Phe), since it displays an n_{app} for E4P of 3.8 (*7*), closely approaching the number of binding sites ($n = 4$). It is relevant that, although there is positive cooperativity for PEP utilization by DAHPS(Phe) (n_{app}=1.4), no cooperativity in PEP binding was found in equilibrium binding studies (*17*).

Table 1: Effect of Tryptophan on E4P and PEP Kinetic Parameters[a]

	erythrose-4-phosphate			phospho*enol*pyruvate		
[Trp] (μM)	V_{max} (μmol min^{-1} mg^{-1})	n_{app}	$S_{0.5}$ (μM)	V_{max} (μmol min^{-1} mg^{-1})	n_{app}	$S_{0.5}$ (μM)
0	33.5 ± 0.5	2.55 ± 0.14	35.0 ± 0.7	30.2 ± 0.4	2.15 ± 0.09	5.3 ± 0.1
0.3	29.4 ± 0.3	2.18 ± 0.07	29.7 ± 0.8	28.5 ± 0.5	2.0 ± 0.1	6.4 ± 0.1
1	24.5 ± 0.4	1.86 ± 0.09	29.2 ± 0.6	23.2 ± 0.4	1.8 ± 0.1	5.13 ± 0.08
5	17.7 ± 0.4	1.38 ± 0.07	29.1 ± 0.5	16.8 ± 0.3	1.60 ± 0.08	5.05 ± 0.08
20	14.2 ± 0.3	1.37 ± 0.07	27.6 ± 0.5	14.9 ± 0.1	1.68 ± 0.06	4.21 ± 0.08

[a] Asymptotic standard errors are from nonlinear regressional curve fitting of velocity data to the Hill equation.

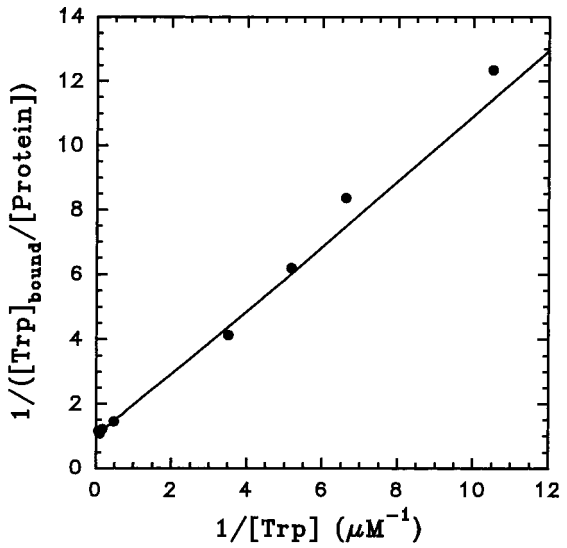

FIGURE 5: Langmuir plot of tryptophan binding by DAHPS(Trp). Tryptophan binding was determined by partition ultrafiltration as described in Materials and Methods. DAHPS(Trp) was at 5 μN (subunit concentration).

Several mechanisms other than simple binding interactions have been proposed as the basis for positive cooperativity in substrate kinetics (*18*). One possibility is that binding of a substrate molecule at one catalytic site of an oligomeric enzyme can affect the catalytic ability of another site through steric or electronic changes. Subunit interactions that increase the rate constants for subsequently binding substrate molecules would result in positive cooperativity, and the kinetic curves would deviate from direct-binding curves for the same substrate. Such "catalytic cooperativity" could explain both the high n_{app} values for E4P and PEP observed with DAHPS(Trp) and the differences between PEP kinetics and PEP binding of DAHPS(Phe). The fact that tryptophan decreases the observed cooperativity for E4P while concomitantly decreasing k_{cat} also suggests the observed cooperativity is associated with catalysis.

Quaternary structure changes affecting catalytic ability can also account for apparent cooperativity in the substrate kinetics of an enzyme. This possibility has not yet been rigorously tested with DAHPS(Trp), but the atypical fractionation behavior of the enzyme during size exclusion chromatography (*6*) suggests the possibility of an equilibrium between active dimeric and inactive or less active monomeric forms. It might also be possible that the changing ratio between metal and substrate in the kinetic experiments contributes to the apparent cooperativity, although there are presently no data to suggest such an interaction.

Inhibition Kinetics. The partial inhibition of DAHP(Trp) by tryptophan may be a metabolic mechanism that has evolved to ensure a basal level of DAHP synthesis under conditions of aromatic amino acid sufficiency. Since inhibition of the DAHPS(Tyr) and DAHPS(Phe) isozymes by their respective feedback effectors is essentially complete, the partial inhibition of DAHPS(Trp) could provide for the continued synthesis of folates, quinones, and other aromatic derivatives of the shikimate pathway (*3*). The maximal inhibition determined here with homogeneous Mn^{2+}-DAHPS(Trp) (*i.e.*, 61%) is similar to that reported earlier with different preparations of the enzyme assessed under conditions of metal heterogeneity (*4*, *5*, *6*, *12*). Thus, it appears that the maximum inhibition is not significantly modulated by the species of activating metal. The $I_{0.5}^{Trp}$ of Mn^{2+}-DAHPS(Trp) determined here (1.4 μM) is slightly less than that reported for metal-heterogeneous enzyme assayed with Fe^{2+} (2 μM) (*6*). This is consistent with earlier findings with DAHPS(Phe), where changes in the activating metal lead to significant differences in $I_{0.5}$ (*7*). Interestingly, the K_i^{Trp} for anthranilate synthase [1.3 μM (*19*)], the main target for feedback regulation of the tryptophan biosynthetic pathway, is nearly identical to the $I_{0.5}^{Trp}$ for DAHPS(Trp), suggesting that feedback inhibition in the two enzymes may have evolved such that they are able to respond to similar intracellular concentrations of tryptophan.

The partial inhibition displayed by DAHPS(Trp) complicates the determination of the mechanism of inhibition. The simplest mechanism for partial inhibition, in which binding of tryptophan to one subunit prevents subsequent binding to the second subunit, is excluded by the results of the direct binding experiments, which indicate independent binding sites (Figure 5). Since enzymatic activity is not completely inhibited by saturating concentrations of tryptophan, models describing inhibition of the enzyme must incorporate an active enzyme−substrate−inhibitor complex. System C5 hyperbolic mixed-type inhibition (*10*) is a compatible model with respect to E4P. In this inhibition system, binding of inhibitor slows the rate of product formation while decreasing the dissociation constant for substrate. Consequently, at low concentrations of substrate, the increased substrate affinity afforded by inhibitor binding leads to an increased rate of product formation, as was observed here with E4P as variable substrate. In contrast, the kinetics of inhibition with respect to PEP appear to be partial, noncompetitive in nature. Increasing concentrations of tryptophan lowered V_{max} while having no significant effect on $S_{0.5}^{PEP}$.

No apparent cooperativity in tryptophan inhibition of the DAHPS(Trp) isozyme was found in this study. This differs from the results of previous studies with the DAHPS(Trp) of *Streptomyces rimosus* (*20*), as well as with the *E. coli* DAHPS(Phe) (*7*, *21*) and *Salmonella typhimurium* DAHPS(Tyr) (*22*). On the other hand, as found previously with DAHPS(Phe) (*7*), the apparent homotropic cooperativity of DAHPS(Trp) for E4P decreased with increasing concentra-

tions of feedback effector. This suggests that a similar mechanism for feedback inhibition may be operating in both *E. coli* isozymes and excludes a concerted Monod−Wyman−Changeux mechanism for the allosteric response.

Substrate Ambiguity in DAHPS(Trp). *E. coli* DAHPS-(Trp) appears to be comparatively very discriminating in its utilization of sugar substrates. Of nine sugars tested, only D-ribose-5-phosphate serves as an alternate substrate for E4P *in vitro*. This is in contrast to numerous plant cytosolic DAHP synthases, which have been found to display a high degree of substrate ambiguity with respect to E4P (*23*). The relatively poor utilization of ribose-5-phosphate by DAHPS-(Trp) is probably not of physiological significance. However, this observation, together with the finding that erythrose was not a productive substrate, indicates the phosphate group of the sugar substrate is critical for productive binding and catalysis.

REFERENCES

1. Brown, K. D., and Doy, C. (1966) *Biochim. Biophys. Acta. 118*, 157−172.
2. Ogino, T., Garner, C., Markley, J., and Herrmann, K. M. (1982) *Proc. Natl. Acad. Sci. U.S.A. 79*, 5828−5832.
3. Herrmann, K. M. (1983) in *Amino Acids: Biosynthetic and Genetic Regulation* (Herrmann, K. M., and Somerville, R. L., Eds.) pp 301−322, Addison-Wesley Publishing Co., Inc., Reading, MA.
4. Pittard J., Camakaris, J., and Wallace, B. (1969) *J. Bacteriol. 97*, 1242−1247.
5. Camakaris, J., and Pittard, J. (1974) *J. Bacteriol. 120*, 590−597.
6. Ray, J. M., and Bauerle, R. (1991) *J. Bacteriol. 173*, 1894−1901.
7. Stephens, C. M., and Bauerle, R. (1991) *J. Biol. Chem. 266*, 20810−20817.
8. Baasov, T., and Knowles, J. (1989) *J. Bacteriol. 172*, 6155−6160.
9. Lee, H., and Wilson, I. (1971) *Biochim. Biophys. Acta 242*, 519−522.
10. Segel, I. (1975) *Enzyme Kinetics. Behavior and Analysis of Rapid Equilibrium and Steady-state Enzyme Systems*, John Wiley & Sons, Inc., New York.
11. Sophianopoulos, J. A., Durham, S. J., Sophianopoulos, A. J., Ragsdale, H. L., and Cropper, W. P. (1978) *Arch. Biochem. Biophys. 187*, 132−137.
12. Ray, J. M., Yanofsky, C., and Bauerle, R. (1988) *J. Bacteriol. 170*, 5500−5506.
13. Atkinson, D. E. (1966) *Annu. Rev. Biochem. 35*, 85−124.
14. Freifelder, D. (1976) *Physical Biochemistry: Applications to Biochemistry and Molecular Biology*, W. H. Freeman and Co., San Francisco.
15. Holtzclaw, W., Chapman, L., and Gowans, C. (1972) *Biochim. Biophys. Acta 268*, 562−572.
16. Jensen, R. A., and Trentini, W. (1970) *J. Biol. Chem. 245*, 2018−2022.
17. Park, O., and Bauerle, R. Unpublished experiments.
18. Neet, K. E. (1980) *Methods Enzymol. 64*, 139−192.
19. Caligiuri, M. G., and Bauerle, R. (1991) *Science 252*, 1845−1848.
20. Stuart, F., and Hunter, I. S. (1993) *Biochim. Biophys. Acta. 1161*, 209−215.
21. Simpson, R. J., and Davidson, B. E. (1976) *Eur. J. Biochem. 70*, 493−507.
22. Nagano, H., and Zalkin, H. (1970) *Arch. Biochem. Biophys. 138*, 58−65.
23. Doong, R., Gander, J., Ganson, R., and Jensen R. (1992) *Physiol. Plant. 84*, 351−360.

BI971135T